Journal of Location Based Services
Vol. 0, No. 0, January 0, 1–21

Molé: a Scalable, User-Generated WiFi Positioning Engine

Jonathan Ledlie*† Jun-geun Park‡, Dorothy Curtis‡,
André Cavalcante**, Leonardo Camara**, Afonso Costa**, and Robson Vieira**

† Nokia Research Center, 4 Cambridge Center, Cambridge, USA
‡ Computer Science and Artificial Intelligence Laboratory, Massachusetts Institute of Technology, Cambridge, USA
** Nokia Institute of Technology, Manaus, Brazil

(*Received 00 Month 200x; In final form 00 Month 200x*)

We describe the design, implementation, and evaluation of Molé, a mobile organic localisation engine. Unlike previous work on crowd-sourced WiFi positioning, Molé uses a hierarchical name space. By not relying on a map and by being more strict than uninterpreted names for places, Molé aims for a more flexible and scalable point in the design space of localisation systems. Molé employs several new techniques, including a new statistical positioning algorithm to differentiate between neighboring places, a motion detector to reduce update lag, and a scalable "cloud"-based fingerprint distribution system. Molé's localisation algorithm, called Maximum Overlap (MAO), accounts for temporal variations in a place's fingerprint in a principled manner. It also allows for aggregation of fingerprints from many users and is compact enough for on-device storage. We show through end-to-end experiments in two deployments that MAO is significantly more accurate than state-of-the-art Bayesian-based localisers. We also show that non-experts can use Molé to quickly survey a building, enabling room-grained location-based services for themselves and others.

Keywords: Crowd-sourcing, WiFi positioning, localisation

1 Introduction

The ability for a mobile device to perceive a user's location has many applications, from social networking "check-ins" to location-appropriate content, such as automatically presenting people with a relevant train schedule.

While the global positioning system (GPS) enables devices to sense their location in most outdoor environments, bad weather and "urban canyons" can restrict its operation. In addition, there are many indoor positioning applications where GPS can provide only limited assistance, as it typically provides a position fix only near windows and doors.

To enable room-grain indoor and outdoor positioning in GPS-less environments, researchers have used physically-fixed wireless beacons to associate a unique "fingerprint" with each place or grid point (Bahl and Padmanabhan, 2000; Priyantha *et al.*, 2000; Haeberlen *et al.*, 2004). While the types of wireless beacons have varied over time, most techniques now use 802.11 WiFi beacons because of their near ubiquity, particularly in urban and suburban environments. Because of the difficulty in translating between distance and received signal strength (Pahlavan *et al.*, 1998), more compact alternatives to fingerprinting – e.g., triangulating among the beacons – are generally eschewed.

One of the key problems with fingerprinting, however, is learning the fingerprint for each place – however "places" are designated. We call the process where a person links a fingerprint to a place "binding." Several commercial vendors offer positioning services, which include a fingerprint-generation survey (Ekahau). However, these come at a steep price: a large office building can cost \$10,000 USD with no maintenance included. Because this is prohibitively expensive for many applications – such as contextualising a device's behavior based on which room of a house it is in – several research systems have begun to crowd-source

*Corresponding author. Email: jonathan.ledlie@nokia.com fingerprints from end-users (Bhasker *et al.*, 2004; Bolliger, 2008; Barry *et al.*, 2009; Park *et al.*, 2010). In the model for these Wikipedia-style approaches, a single locally-knowledgeable user performs the bind for a place and many visitors can then rely on the database of fingerprints.

Molé focuses on a new point in the design space of these crowd-sourced, or "organic," positioning systems. Some systems, such as OIL (Park *et al.*, 2010), present a map to the user: users bind places by clicking on the map. Others, like Redpin (Bolliger, 2008), allow the association of any text string with a place's fingerprint. In contrast, Molé arranges the world hierarchically; this imposes a clean, intuitive namespace (country, region, ...), and allows for data prefetching at a building scale if not larger. It also isolates problems in the fingerprint database to small portions of the tree. Molé relies on compact data structures that allow many fingerprints to be stored on the user's device. In turn, this allows the user's device – not a server – to select among potential places with similar fingerprints, improving privacy.

Here we describe how Molé's hierarchical namespace leads to a scalable design, where its servers can be easily replicated in the "cloud." We show how its new statistical positioning algorithm uses response rate as additional fingerprint information. In our experiments, this leads to an improvement in accuracy of 10% over the current state-of-the-art. We also show how Molé uses accelerometer-based motion detection both to reduce the latency in showing the correct place after a user has moved and to collect clean fingerprints from end-users. Through a crowd-sourcing experiment, we show that a multi-story building can be quickly and accurately covered by non-experts: in one hour, four people completely surveyed a mid-sized research lab. After this surveying period, which can be concurrent with use, any person visiting the lab can benefit from room-customised behavior, from location-aware assistance and notifications to device and application contextualization.

This article's contributions are:

- A new organic positioning system, called Molé, whose positioning algorithm explicitly accounts for temporal variations in the signal space;
- A detailed description of Molé's hierarchy of places and cloud-based, batch design;
- A simulation and experimental analysis of Molé, including crowd-sourcing a multi-floor building with untrained users;

The article, which focuses on Molé's positioning algorithm, proceeds as follows. We describe and show the user interface for the place hierarchy in Section 2. We outline our positioning algorithm in Section 3. In Section 4, we show how Molé's architecture takes advantage of the "cloud," to allow fingerprints to be combined efficiently and for clients to receive the contributions of others quickly. In Section 5, we describe our evaluation of Molé, examining its positioning algorithm versus the current state-of-the-art, its use of movement detection, and how end-users can use it to build up a working deployment in a multi-story building. We describe related work in Section 6 and conclude in Section 7.

2 Model of Places

Molé arranges the discrete, human-designated places of the world in a hierarchy. While the hierarchy could be of variable depth, our current implementation contains five levels, as the estimate in Figure 1 illustrates. From coarse to fine, the levels typically refer to country, region, city, area, and unique place (e.g. room). Areas are the unit of fingerprint aggregation, transfer, and, therefore, privacy; the server knows at most what areas you visit. Areas typically refer to street addresses (e.g., "4 Cambridge Center" in Figure 1), although they could refer to larger outdoor areas such as parks. The design also allows aggregation at higher levels.

We believe that arranging places in a hierarchy is useful in many organic positioning settings. Earlier approaches have used visual maps (Bhasker *et al.*, 2004; Park *et al.*, 2010) or uninterpreted strings (Bolliger, 2008) to identify individual places. Visual maps require that a fairly accurate map of the area – typically a building – exists. While well-managed places, such as universities and airports, may be able to generate maps, this approach may not scale to individual homes or businesses, where people may not have the time, knowledge, or interest to create a map of their sets of places. In addition, many users find it non-trivial to locate themselves on indoor maps, particularly in complex buildings. Assigning uninterpreted strings

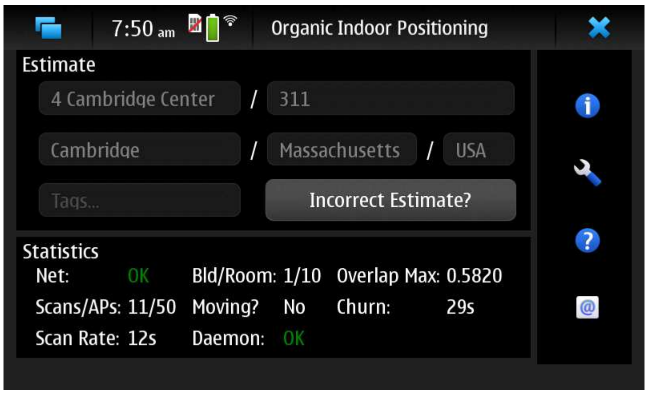
7:50 am Organic Indoor Positioning

Estimate

4 Cambridge Center / 311

Cambridge / Massachusetts / USA

Tags... Incorrect Estimate?

Statistics

Net: OK Bld/Room: 1/10 Overlap Max: 0.5820

Scans/APs: 11/50 Moving? No Churn: 29s

Scan Rate: 12s Daemon: OK

Figure 1. **Molé's User Interface.** It shows the country, region, city, area, room hierarchy in street address format. The statistics shown are described in Section 4.1.

to places during a bind has its own challenges: for example, the namespace may rapidly become crowded with similar names. While Barry *et al.* (2009) do allow for spaces within buildings, their hierarchy is not intended to cover the world.

Figure 1 shows the current estimate of a device's position within this hierarchy. While the depth and names of the hierarchy are currently predefined, different countries or cultures could change its shape as they saw fit, assuming the user interface could handle this variation. Users click on the "Incorrect Estimate?" button to edit the current estimate and make a new bind, improving future estimates for themselves and other users. The statistics are explained in Section 4.

3 Algorithm

In this section, we describe our new, statistical localisation algorithm (§ 3.1), briefly review naïve Bayesian localisation (§ 3.2), and describe a kernelised RSSI histogram variation that can be applied to both localiser types (§ 3.3).

3.1 *Maximum Overlap Localisation*

Maximum Overlap, or MAO, selects its estimated place as the one whose fingerprint is most similar to the user's fingerprint, using a similarity function we describe below. MAO has two key advantages. First, it is efficient to compute. Because we anticipate localisation algorithms running continuously in the background on mobile devices, this simple computation should translate into longer battery life. Second, it provides a scan distance function, which can be used to estimate physical distances between sets of fingerprinted objects. Scan distance functions are also useful for clustering scans, outlier detection, and cleaning scan databases (citation: park10growing). By themselves, distance functions are also useful for estimating the physical distance between the positions where the scans were made, which we show in Section 5.4.

To create a MAO fingerprint, we begin with a standard set of place-to-APs histograms containing raw RSSI readings. As in Haeberlen *et al.* (2004), we summarise each per-place per-AP histogram with a single Gaussian with mean μ and standard deviation σ (we describe a kernelised histogram variant in § 3.3).

Every place is assigned a fingerprint, which is a set of mappings from access points to data triples:

$$AP_i \Rightarrow \langle w_i, \mu_i, \sigma_i \rangle \tag{1}$$

where w_i is the weight of AP_i, the number of observable APs is τ, and the total weight for each fingerprint $\sum_{i=1}^{\tau} w_i$ is 1. Note that the most recent k scans of the user also form a fingerprint using the same method.

Determining the weight w to apply to each visible AP is an important component of our algorithm. A straw man method would be to simply weigh each visible AP equally: $1/\tau$. Instead, we base the weight on the probability that the given AP will actually be observed in the place. Specifically, we set the probability to the response rate, the fraction of a fingerprint's scans in which a given AP was observed. When a place is scanned many times, some APs will be seen in every scan, and some seen only rarely. This captures the intuition that a user's device will see the same APs with the same signal strength distribution *and* the same observation frequency when it is in the same place (these two quantities are only weakly correlated as we show in Section 5.1). If the user's fingerprint does not contain an AP that is almost always observed when in a particular place, it is highly unlikely that the user is in this place. Weighting according to response rate reflects this intuition. Specifically, the weight for AP_i is:

$$w_i = r_i / \sum_{j=1}^{\tau} r_j \tag{2}$$

where r_i is the number of readings of AP_i.

To find the similarity between two fingerprints, we determine the similarity in signal strengths of APs that exist in both fingerprints, and penalise for missing APs, weighting both quantities by the response rate. The comparison of any two fingerprints returns a similarity $-2 \leq S \leq 1$, where a comparison of identical fingerprints returns 1 and of disjoint fingerprints returns -2 (Disjoint fingerprints are those that share no access points). For fingerprints A and B:

$$S(A,B) = \sum_{i \in A \cup B} \delta_i \tag{3}$$

where δ_i is the effect each AP_i. This delta of each AP is computed as:

$$\delta_i = \begin{cases} \frac{\omega_a + \omega_b}{2} \times O\left(\mu_a, \sigma_a, \mu_b, \sigma_b\right) & \text{if } i \in A, i \in B, \\ -\omega_a \times p & \text{if } i \in A, i \notin B, \\ -\omega_b \times p & \text{if } i \notin A, i \in B, \end{cases} \tag{4}$$

where $O(\cdot)$ is the overlap coefficient between the two Gaussian distributions (Inman and Bradley, 1989) and $0 \leq p \leq 1$ is the penalty to apply for missing APs.

Figure 2 provides an example of computing the similarity between a pair of fingerprints. The example shows two places (top and middle) and the overlap of their fingerprints (bottom). The 20 scans in $place_1$ have sensed three different access points: AP_1, AP_2, and AP_3. The 25 scans in $place_2$ have only sensed two access points, both of which are the same as those seen in $place_1$: AP_1, AP_2. AP_3 was not observed in $place_2$. To compute the weights for $place_1$, we divide the observations for each AP by the total number of observations, $20 + 15 + 5 = 40$. The same procedure is done for $place_2$. This completes the creation of fingerprints for these two places. The bottom row shows how the similarity between the two fingerprints for places 1 and 2 is computed:

$$s = 0.75 \times \frac{20/40 + 25/45}{2} + 0.30 \times \frac{15/40 + 20/45}{2} - 5/40 \tag{5}$$

where the penalty $p = 1$, and 0.75 and 0.30 are the overlap coefficients for AP_1 and AP_2, respectively. "$Place_2$" could equivalently be a set of scans as seen by a user's device: the algorithm to compute their similarity would be the same. Because the same comparison applies whether place B is a user's fingerprint or any collection of scans – such as a location tag – it can be used to estimate a physical distance between two real or virtual objects (e.g. virtual graffiti).

One particularly nice aspect of this overlap computation is that it exists as a closed-form function when Gaussians are used to represent the RSSI readings (Inman and Bradley, 1989). Alternatively, the results from the function can be stored in a look-up table (Linacre, 1996); we found a table with only hundreds of values gave almost the same results as a function. This simple computation is in contrast to graphical models (Madigan *et al.*, 2005), which may require thousands of iterations to converge.

A special case exists where we have only a few RSSI measurements for an AP. In particular, the sample variance, which is a second-order statistical property, is not well-defined with only one sample. Because

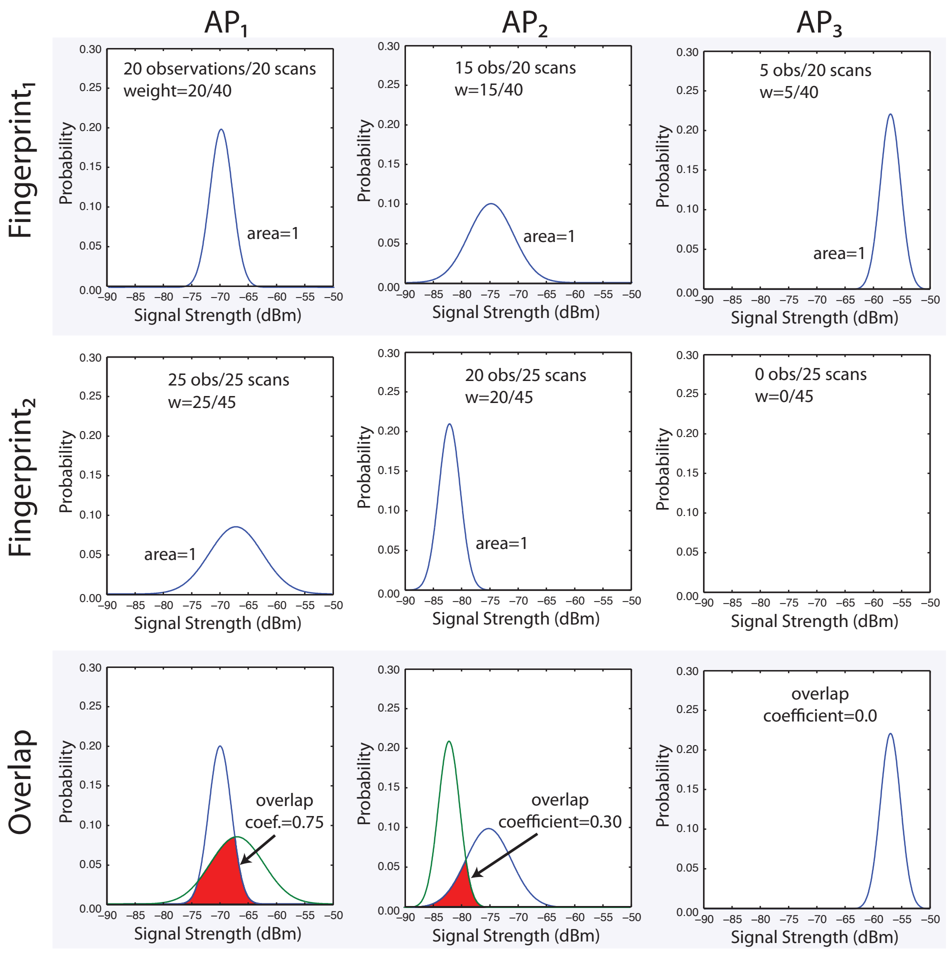

Figure 2. Example of computing the similarity between two fingerprints using MAO: $place_1 \cup place_2$ = Overlap.

this situation by definition exists for rarely observed APs, taking more scans is not advisable as we may need to take many more in order to obtain a stable estimate for σ. Instead, to estimate σ for these APs, we use a weighted average of this AP's sample standard deviation σ_s (if it exists) together with a common prior σ_c:

$$\sigma_i = \frac{(r_i - 1)\sigma_s + \sigma_c}{r_i} \tag{6}$$

With this, the overlap coefficient can be computed even with very few RSSI values, or even a single value, from a given AP. We found $\sigma_c = 1$ worked well in our experiments.

3.2 *Naïve Bayes Localisation*

We compare MAO to state-of-the-art naïve Bayes localisation in Section 5.2. For completeness, we briefly review Bayes localisation here (for more detail, see Haeberlen *et al.* (2004) and Madigan *et al.* (2005)). Bayesian localisation estimates the most likely location using Bayes' rule. Naïve Bayes localisation further assumes that the signal strengths from different access points are independent from each other given a location. Therefore, given a signal strength vector $s = [s_1, s_2, ..., s_k]$ from k access points, the posterior probability of being in location l is given by

$$P(l|s) = \frac{\prod_i^k P(s_i|l)\ P(l)}{P(s)}. \tag{7}$$

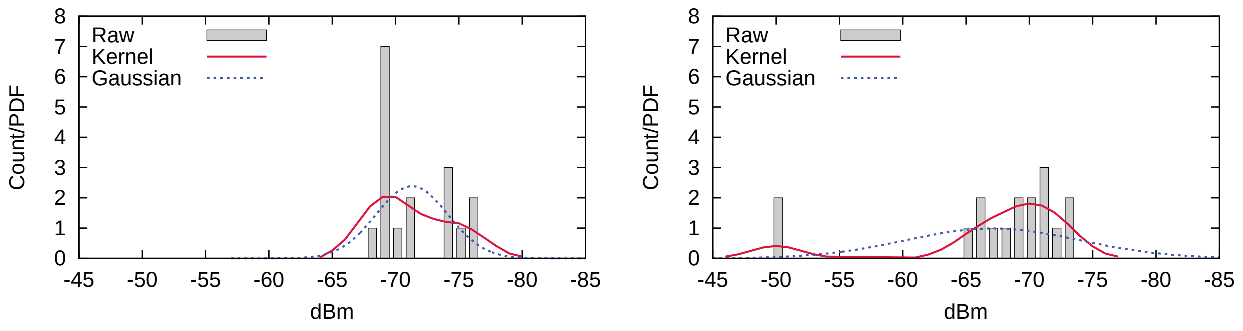

Figure 3. RSSI histograms and their kernel and Gaussian representations, taken from two APs seen in the same bind. The left figure shows how the peaks of a "narrow" bimodal can be more accurately captured by a kernel representation. The right figure shows how a Gaussian can artificially spread out a bimodal that has two distant peaks.

Since P(s) is fixed given the observed signal strength vector s, With a uniform prior assumption on $p(l)$, the final location estimate $\hat{l}$ is given as follows:

$$\hat{l} = \underset{l}{\operatorname{argmax}} \left[\prod_{i}^{k} P(s_i|l) \right]. \tag{8}$$

Previous work has compared similarity and nearest neighbor-based approaches to Bayesian ones and come to differing conclusions (Youssef and Agrawala, 2005; Dong *et al.*, 2009). The main generalizable aspects that MAO adds to previous work are (1) its use of a weighting factor that values the effect of APs differently and (2) its penalisation for missing APs. Foreshadowing our results, we find in Table 1 that two performed equally without these techniques (columns two and six). Bayesian localisation has the advantage that it is natural to include prior estimates through a non-uniform valuation of $P(l)$, making it less likely that an estimate will "jump" across a building for example. While we study these generalizable aspects in the context of MAO, we invite other researchers to apply them to Bayesian localisers.

3.3 *Kernelising RSSI Histograms*

A final algorithmic technique that we have tested in Molé is kernelising RSSI values – essentially spreading a given reading over adjacent bins – a technique Park *et al.* (2011) used for sharing fingerprints across heterogeneous devices. The key observation is that summarising a set of RSSI values with a Gaussian can often lead to Gaussians that are similar across nearby rooms. The alternative to a Gaussian summarisation has typically been to simply leave the RSSI values in raw histogram form. For example, a fingerprint based on histograms might include five -78 dBm readings, three -80 dBm, and one -83 dBm reading from a particular access point. By leaving these values in raw form, a reading of e.g. -79 dBm will be discounted, instead of contributing to a match as it should. A Gaussian summarisation, however, will also not yield an accurate picture for the distribution's shape: it is skewed toward -78. Instead, as shown in Figure 3, we can apply a kernel to each RSSI value, effectively spreading it out into adjacent bins without affecting the overall shape. This shape can capture differences between neighboring spaces that would be blurred by a Gaussian summary.

Another advantage of the kernel representation of fingerprints is that it makes a method for sharing fingerprints across heterogeneous devices (Park *et al.*, 2011) applicable to MAO as well. As different RF devices have different signal characteristics both at the hardware and software level, a set of RSSI fingerprints captured from one type of device will not produce highly accurate localisation when used unaltered on another type of device. To reduce the fingerprint difference between heterogeneous devices, Park *et al.* (2011) applied a linear transformation of signal strengths followed by kernelisation of the RSSI histogram. When applied to MAO, this kernelisation yields a similarity score more reliable across different devices, because it makes the individual difference of noise characteristics less distinct across devices.

One issue with using histograms as compared to Gaussians is the requirement that – in theory – they consume an order-of-magnitude more space. This increase in space consumption is due to the range of RSSI values (typically -30 to -100 dBm) versus a simple mean and standard deviation. Multiplied by many places and many access points, this space consumption arguably could be significant for on-device positioning. In practice, however, because so few bins of the histogram are used – even when kernelising – that the actual space consumption is only a few floating point numbers more per access point in our experience.

Histogram kernelisation can be applied both to similarity-based localisers like MAO and to Bayesian localisers. We compare the accuracy of Bayes and MAO with and without kernelised histograms in Section 5.2.

4 Implementation

Molé's implementation is divided into client and server components. The client portion periodically scans WiFi signals and makes an estimate of the current place available to other applications on the same mobile device. Because all position estimates are calculated on the client using a cache of fingerprints, the client's exact position remains private and new estimates can be made in the absence of network connectivity. The server can only know which aggregations of fingerprints have been requested, not which rooms have actually been visited.

4.1 *Client Components*

The client itself consists of two parts: a daemon, which runs continuously in the background, and a user interface, which is displayed when the user wants to make a bind, modify the daemon's behavior, or view statistics. Figure 1 shows the user interface. Its statistics include: the number of scans being used to form the estimate; the count of distinct APs that were observed within these scans; the current time between scans (*i.e.* scan period); the number of areas and individual places within those areas under MAO consideration; whether the user is deemed to be moving; the score of the current estimate ("overlap max"); and churn, the time since the estimate was last changed. The Molé daemon exports the current location estimate to all applications on the device, assuming that the user has set "sharing" to be on.

4.1.1 ***Using Motion Detection.*** As Haeberlen *et al.* (2004) showed, comparing more user scans against each fingerprint improves spot-on accuracy, with diminishing returns after about eight scans with their data. But frequent scanning reduces battery life, and having a fixed, large number of user scans introduces a lag when the user is moving between places. If a device has an accelerometer, Molé uses it to find a happy medium between battery consumption and update lag. If the device is estimated to be stationary, it slows down the scan rate and other functions. When walking is detected, the current set of user scans is discarded and the scan rate is increased (up to once per 10s in our current implementation). By truncating the user scans (11 in Figure 1), Molé returns a less accurate, but more timely estimate. When the user stops moving, the user scans accumulate and the accuracy of the estimate improves. Because we simply truncate the positioning and bind queues in response to movement, our method is independent of the choice of the particular motion detection algorithm; we use Shafer and Chang's detector (Shafer and Chang, 2010). An alternative method would treat the detector as less of a black box and could dynamically adjust the length of the queues based on the magnitude or confidence with which movement was detected. To further reduce battery usage, we run the motion detector every 10 seconds with a duty cycle of 5%; at this rate motion detection has little effect on the overall battery consumption of a typical smartphone. We evaluate the effect of using motion detection on update delay and fingerprint creation in Section 5.3.

4.1.2 ***Client-side Filtering and Positioning.*** Client localisation involves fetching the correct area's fingerprint file (if it is not cached on-device), filtering down to a few fingerprints to be tested more precisely, and producing a top estimate with MAO. As shown in Figure 4, the client periodically asks the server for the

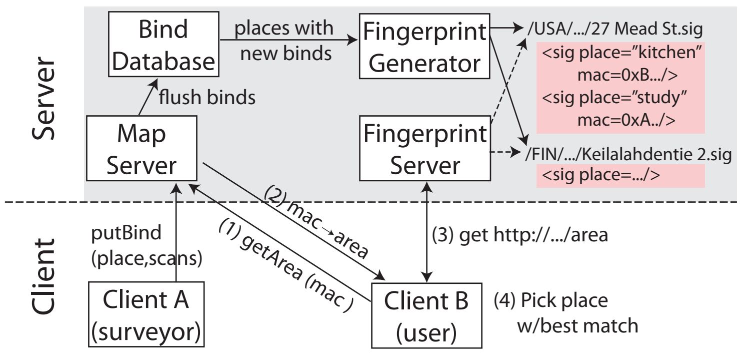

Figure 4. Interaction between Molé's client and server components. Two paths are shown: (a) a bind coming from a surveyor (client A), being added to the bind database, and being processed into an area's fingerprint file (e.g. Keilalahdentie 2.sig) and (b) a user's device (client B) updating its local cache of fingerprints for the areas that it is potentially in. First it queries to see which areas match a random "loud" MAC with `getArea()`, then it fetches the fingerprint files for those areas. After its cache is up-to-date, it can form a position estimate locally.

list of areas associated with one of its visible MACs (step 1), and receives the fully-qualified (hierarchical) area name in response (step 2). It then requests the area's fingerprint file (step 3) and localises using the current user scans (step 4). To reduce the number of fingerprints that MAO must compare, we apply Charrow's fingerprint filtering to our local cache to identify a set of "nearby" locations (Charrow, 2010); in Figure 1, ten places have passed this filter. We use the filter twice: first on the cached areas, then on the cached places within the unfiltered areas. Because areas can contain many places, this greatly reduces the number of places that must be compared when many areas are cached on the device. In addition, because the filter uses only MAC presence/absence, it is far less CPU intensive than a room-level localiser. The more CPU intensive MAO then runs on the smaller subset of places that have successfully passed the area and place filtering steps. Like other room-level localisers, MAO's CPU usage is linear in the number of potential places under consideration, so reducing the set under its consideration can reduce battery consumption considerably when many places are cached.

4.2 *Server Components*

Figure 4 shows Molé's four main server components and the key methods clients use to make binds and access fingerprints. Molé's server side is designed to run elastically "in the cloud:" its client-facing components, the Map Server and Fingerprint Server are easy to replicate. The figure shows the two paths of client actions: (a) binding and (b) localising. A client bind is sent to the Map Server, which acts as a write-back cache. The Fingerprint Builder periodically monitors the database for places with new binds (or entirely new places). For each of these places, it aggregates all recent binds and determines a new fingerprint. Fingerprints for other places in the same area are cached in the database. The builder then writes out each changed area's collection of fingerprints in a single area fingerprint file. Because these files change infrequently and are named by the fully-qualified area, they can be trivially cached, versioned, and compared.

Molé's server components are currently hosted on Amazon Web Services [1]. While we show only one server instance in the figure, it is fairly trivial to replicate and scale the server components because they can be divided geographically; that is, the bind database, in particular, can be partitioned down to the level of individual areas if need be. Because area fingerprint files change slowly over time after their initial creation period, we serve these files with an efficient static web server. Replicas could be further pushed toward the client with a content delivery network. To receive fingerprints created by other nearby users, clients poll for changes in their current area's fingerprint at one minute intervals.

The source code for Molé has been released under an open source license and we invite contributions [2]. The client components are $\approx 7k$ lines of Qt/C++; the server is written in Java and Perl and relies on

[1] `http://mole.research.nokia.com`
[2] `http://github.com/organic-positioning`

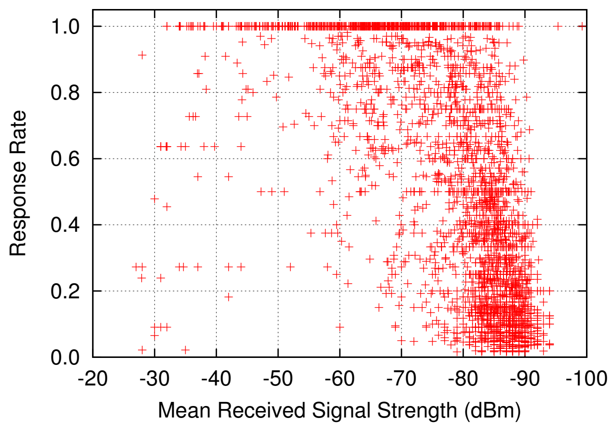

Figure 5. As previous work has found, there exists a moderate correlation between response rate and received signal strength. These data are from 81 Molé binds taken in a variety of indoor environments.

several open source libraries.

5 Evaluation

We have successfully tested Molé in preliminary trials at several labs, using Nokia N900 tablets. Here, we examine Molé in detail, both at the algorithmic and end-user level:

- We find that MAO's weight (based on response rate) and RSSI readings contribute independently to uniquely identifying a place (§ 5.1).
- Through a set of controlled experiments, we find that MAO has favorable accuracy results as compared to a state-of-the-art Bayes localiser, achieving better performance when places are physically adjacent (§ 5.2).
- We show that use of a motion detector can result in a dramatic improvement in update delay and in unpolluted fingerprint creation in organic settings (§ 5.3).
- We show how MAO can be used to estimate the physical distance between two objects (§ 5.4).
- Using the results from a deployment in a two story building, we show that Molé can rapidly crowd-source an accurate location system (§ 5.5).

5.1 *Using Response Rate*

Before we examine Molé's performance, it is reasonable to ask whether it is valid to use response rate as the basis for MAO's weighting factor at all. That is, is the response rate supplying distinct and consistent information as compared with RSSI values, or could one be substituted for the other? Specifically, we ask: (a) Are they redundant quantities? (b) Is response rate consistent over visits to the same space? (c) Do they increase differentiability between different spaces? (d) How does response rate relate to "negative information" e.g. the absence of an AP, and (e) Does the weight improve end-to-end accuracy? We also examine the effect of weight experimentally in Section 5.2.

First, using bind data from different alpha users of Molé, we find that they are not redundant quantities. In Figure 5, we show a scatter plot of the average RSSI value vs. the response rate for the same MAC. The data is from 81 binds from different indoor environments (e.g. labs, houses); *response rate* is the fraction of scans where the MAC was seen in each bind. In this data set, the two are only moderately correlated ($\rho^2 = 0.62$), suggesting that response rate, and therefore Molé's normalised weighting measure, provide additional information beyond received signal strength.

Second, to examine consistency over time, we compared an older set of binds to a newer one for eight rooms in one of our labs. The older set were all generated at least six months earlier than the newer set. Fingerprints in each place contained 31 distinct MAC addresses on average. We found a strong correlation for both response rate ($\rho^2 = 0.73$) and RSSI ($\rho^2 = 0.87$), suggesting that these mainly independent values

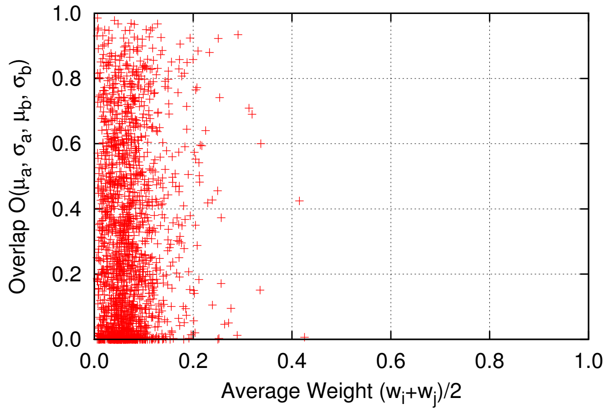

Figure 6. While response rate and received signal strength are moderately correlated (see Figure 5), the average weight $\frac{\omega_a+\omega_b}{2}$ and overlap $O(\cdot)$ only exhibit very low correlation. In this data set, taken from a nine-story building, the two quantities only have $\rho^2 = 0.11$. This lack of correlation suggests that MAO is, in fact, taking advantage of independent sources of information.

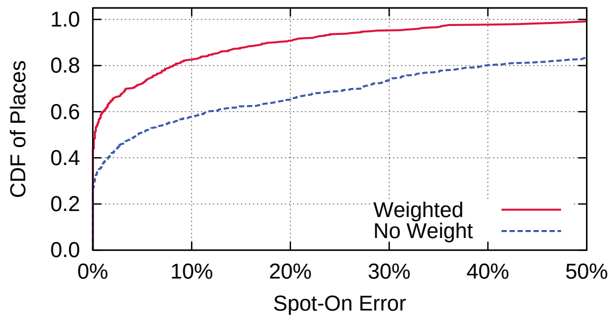

Figure 7. When the weighting functionality is switched off and all RF sources are counted equally, we found greatly reduced accuracy. For example, only 9% of places had an error rate of less than 20% using the weighting function, but 34% had this same level of accuracy without it.

stay consistent over time, and, therefore, can separately assist in identifying individual places.

Third, we examine whether MAO's weight is correlated with RSSI overlap; that is, when comparing across places, is it providing additional, differentiable information. Using a professionally-collected scan data set from a nine-story building which contains more than 1,400 distinct places, we compared the weight $\frac{\omega_a+\omega_b}{2}$ and the overlap $O(\cdot)$ for all MACs in common across places ($\approx$ 150 million entries). When overlap is computed with Gaussians, we find a correlation of $\rho^2 = 0.11$ and, when it is computed using kernelised histograms, that of $\rho^2 = 0.08$. A random sample of the data using Gaussian overlap is shown in Figure 6, illustrating their independence. We also divided the rooms that were close to each other and far away (less than the median distance of 12m or greater than that, respectively), and found the correlation essentially unchanged. Collectively, this set of results suggests that not only are response rate and weight consistent over time, but also that they provide independent information for comparison among places.

Fourth, we discuss the relationship between response rate and what previous work has referred to as "negative information." For example, Letchner *et al.* (2005) use the absence of an AP to bias the estimate in cases where the positive (presence) information is sparse or symmetric. We similarly use the absence of APs to reduce ambiguity between two sets of scans (fingerprints). In MAO's case, we penalize the overlap when APs are missing; Letchner *et al.* solve this by assigning an out-of-range dBm value to the missing APs. What is significantly different is the extent to which we penalize missing APs: if an AP is rarely seen in a given place, MAO only weakly penalizes for its absence; conversely, it penalizes strongly if an AP "ought" to be seen. How often does this occur? If response rates were highly bimodal, then these two approaches would be effectively the same. In Figure 8, we show two distributions of response rates for the same nine-story building, as collected by two different types of devices at different times. The data show that 35-40% of access points had a response rate of $\leq$ 20%. In a short scan on a user's device, there is a reasonable likelihood that these APs would not be sensed. However, they could well be part of the

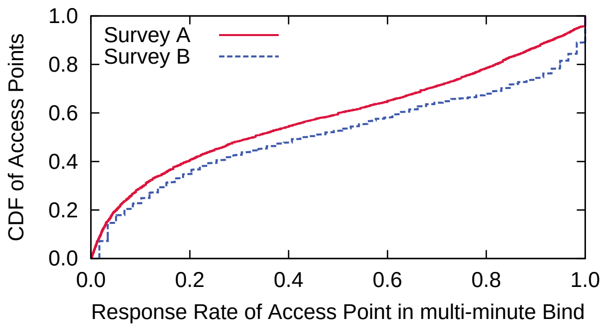

Figure 8. Because response rates range fairly uniformly, penalizing equally for the absence of an AP does not appear to be the best use of "negative information." The figure shows the distribution of response rates of access points from binds lasting several minutes from two surveys of the same nine-story building. Survey A was conducted by a commercial location systems provider using their own proprietary equipment and includes 482 binds. Survey B used Nokia N900s and consists of 47 binds. Response rates across these two surveys was similar and in line with other surveys in other locations.

fingerprint for that same space because the AP is occasionally sensed there (especially if the fingerprint is an aggregation of crowd-sourced scans). Because response rates range fairly uniformly, applying the same penalty for all missing APs too strongly penalizes APs that are unlikely to be observed and too weakly penalizes APs whose presence is expected.

Lastly, we examined the effect of eliminating the weighting factor on positioning accuracy. In simulation, we prepared a scan data set from the same nine-story building as above. We first excluded places with fewer than three visible APs or fewer than ten scans, removing 6% of places. Next we assigned a fingerprint to each place, assuming knowledge of all scans of the place. For each place, we took eight scan samples to build a "user" fingerprint, and then observed which place had the maximum matching fingerprint. If the place the localiser estimated was the same as the user's, this was deemed a spot-on estimate. We repeated this test 1000 times for each place: for example, an accuracy of 80% means that we correctly localised $\frac{800}{1000}$ times. Using the scan trace, Figure 7 shows the effect of weighting according to response rate as compared to weighting each AP equally, *i.e.* setting $w = \frac{1}{\tau}$. While it is possible other refinements exist, such as weighting according to the maximum RSSI value seen for the given AP, it is clear that a reasonable weighting is more accurate than simply valuing all APs equally. In addition to comparing MAO to a Bayesian localiser, we confirm the positive effect of basing a weight on response rate experimentally in the following section.

5.2 *Positioning Algorithms*

To examine Molé's positioning performance in a controlled setting, we conducted three experiments in two different labs, shown in Figure 9. The goal of these experiments is to compare MAO with a state-of-the-art naïve Bayes algorithm, using both Gaussian summaries and kernelised histograms.

In Lab A, we conducted two end-to-end comparisons: a "nearby" experiment and a "distant" experiment. In the "nearby" experiment, the target rooms were adjacent to each other, separated by less than three meters, and had glass walls on one side. In the "distant" experiment, the targets are spread uniformly over the floor. In both experiments, we placed a stationary *spot-check* device in each target room. The spot-check devices did not move throughout the experiment; they polled the server for new fingerprints at one minute intervals, performed scans at ten second intervals, and computed four estimates – one for each algorithm – using the same set of scans and fingerprints at the same time. Another device acted as the roving, crowd-sourcing surveyor. With it in hand, a member of our team walked to 6-8 rooms on the floor, including those being tested, and bound each room with 2-3 minutes worth of scans. The bind data was sent to the server, processed into a fingerprint, and made available for download by the spot-check tablets. The bind database was cleared before each experiment.

Results from the "distant" experiment showed that all of the algorithms were able to perfectly distinguish rooms when the rooms under test were tens of meters apart. Here, the target rooms were R1, R4, and R10, as highlighted in Figure 9a. The mean distance between each of these target rooms and all of the other

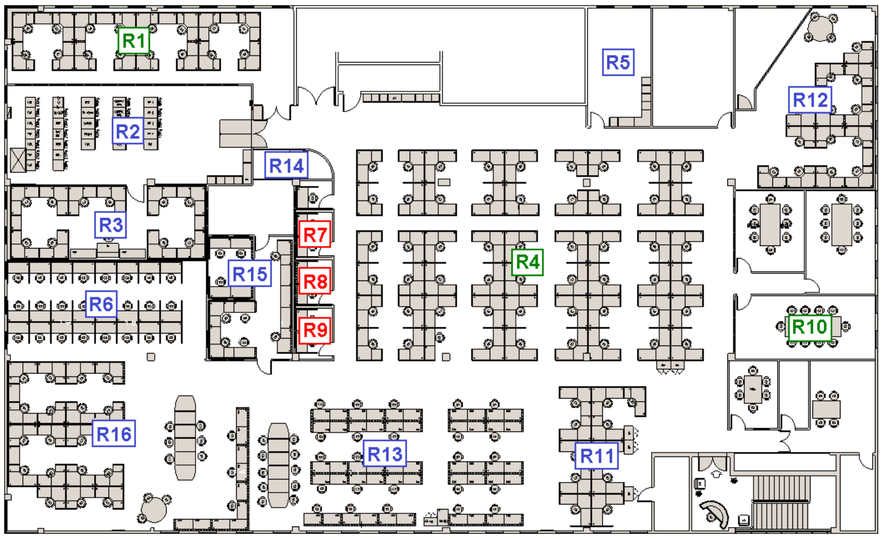

(a) Lab A Third Floor Map. Stationary tablets for "nearby" experiment were placed in R7, R8, and R9 (in red); those for the "distant" experiment were places in R1, R4, and R10 (in green).

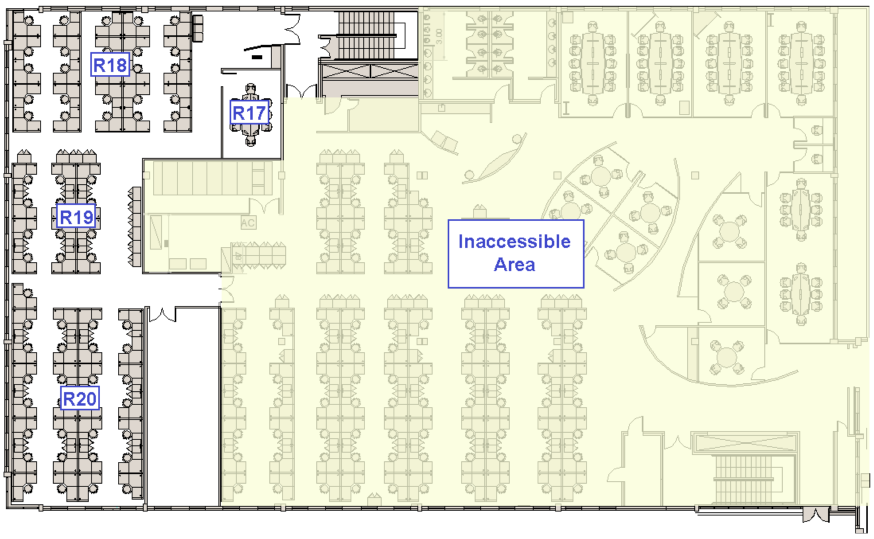

(b) Lab A Second Floor Map. Volunteers spent about 25% of their time on this floor during the crowd-sourcing experiment (§ 5.5).

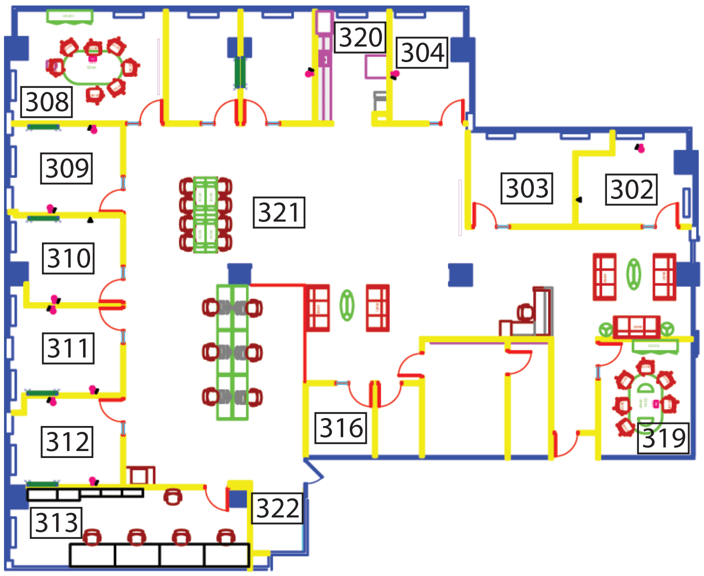

(c) Lab B Map

Figure 9. Floor plans for the two different labs where we conducted experiments.

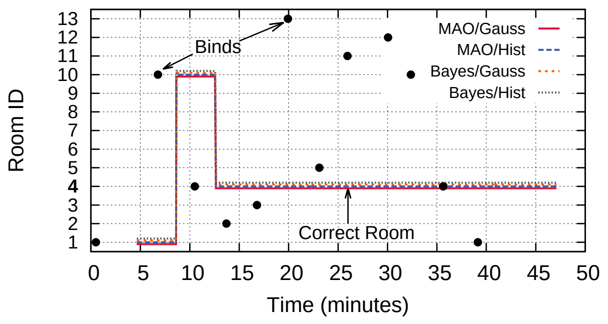

Figure 10. When the locations with fingerprints are tens of meters apart, all of the localisation algorithms were able to successfully select the correct space. The spot-check tablet was located in Room R4. Soon after the roving tablet bound R4, all of the algorithms running on the stationary device in R4 selected it.

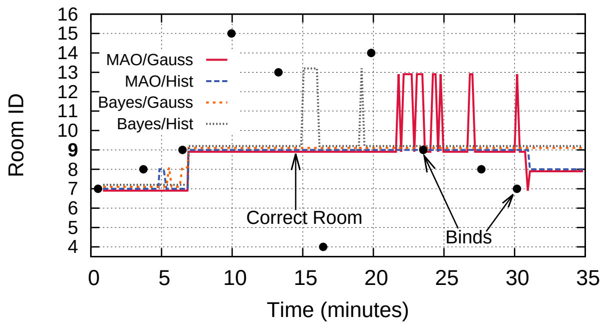

Figure 11. The time series from the "nearby" experiment illustrates how both MAO and Bayes can exhibit instability.

rooms where binds were performed (R2, R3, R5, R11, R13) was 21.59m, 15.90m and 22.59m, respectively. Data from the spot-check tablet in Room R4 are shown in Figure 10. Initially, all devices select Room R1 because that was the only entry in the database. The roving survey tablet binds Room R4 at minute 10. After the spot-check tablet fetches the area's new fingerprint, which now includes R10, all of the algorithms change their prediction to R10. Even with binds in three rooms that are less than 14m away, (R5, R11,R13), the algorithms continue to estimate the correct room to the end of the experiment.

In contrast to the "distant" experiment, the "nearby" one exemplifies the challenges in fine-grain WiFi localisation. The three rooms (R7, R8, R9) are small meeting rooms, each 5.8m^2. They lie in a line with the two end rooms 2.7m from the center one, R8. The entry walls and doors are glass, and join a common hallway. We examined the average spot-on hit rate for each room's stationary tablet, in addition to the mean error and its deviation. The results show that, while Bayes with Gaussians had the lowest mean error for the two end rooms, MAO with kernelised histograms had the best overall performance: its average hit rate was 90.7% while Bayes with Gaussians, the next best, was 68.4%. Two interesting behaviors, in particular, are apparent from examining time-series plots for the stationary tablets. First, MAO is more willing to shift between rooms – sometimes to its advantage, sometimes to its detriment. It does this because it has no hysteresis, or prior, like naïve Bayes does. MAO with Gaussians was particularly unstable in this experiment (see, for example, minutes 22-25 in Figure 11). Second, MAO with kernelised histograms was the only algorithm able to consistently differentiate between the two immediately adjacent spaces; this is what leads it to having the highest average hit rate. From this we conclude that any of the algorithms are acceptable in medium to coarse grained scenarios, as in the "distant" experiment, but that MAO with kernelised histograms may supply the best average-case performance if room-grain accuracy is required.

In Lab B, we had more spot-check tablets available and conducted a larger-scale, longer duration experiment. We first instrumented the tablets to run six localisers in parallel, each producing an estimate using the same set of scans at the same time. In particular, we wanted to see the effect of different parameters for MAO with kernelised histograms in a live setting. Referring to Equation 4, we ran MAO: (a) with *no weight*, treating all APs equally (as in Figure 7) and with no penalty for missing APs, (b) with weight but *no penalty*, weighting APs by response rate, but still without the $-\omega_a \times p$ and $-\omega_b \times p$ factors, and (c)

Table 1. Algorithm Comparison (Lab B) - Spot-On Hit Rate (Floor plan in Figure 9c)

Room	MAO/ Gauss	MAO/ Hist./ No Wt.	MAO/ Hist./ No Pen.	MAO/ Hist./ Penalty	Bayes/ Gauss	Bayes/ Hist
302	92.87	100.00	100.00	100.00	100.00	100.00
303	90.59	100.00	100.00	100.00	74.64	88.52
304	92.09	98.73	100.00	100.00	91.46	79.75
308	99.84	99.84	100.00	100.00	90.49	100.00
309	32.86	42.70	59.37	58.89	31.75	43.33
310	1.59	10.95	41.75	81.59	24.76	11.43
311	90.59	41.15	87.08	94.90	87.56	95.37
312	42.88	93.67	90.03	70.89	70.09	72.47
313	100.00	100.00	100.00	100.00	99.16	100.00
316	100.00	100.00	100.00	100.00	98.73	100.00
319	99.84	100.00	100.00	100.00	98.57	97.14
320	100.00	98.74	100.00	100.00	99.37	100.00
321	99.22	100.00	100.00	100.00	100.00	100.00
322	88.38	100.00	100.00	99.53	92.15	97.33
All	80.46	84.49	91.17	93.16	82.52	84.43

with weight and a *penalty*, where $p = \frac{1}{4}$ (since the tablets were stationary, the motion detector was not a factor). We placed fourteen spot-check devices in different rooms in the lab, including three in public spaces without doors between them (320, 321, and 322 in Figure 9). Using two roving devices, we bound the spaces starting in room 312 and moving clockwise around the lab; each bind contributed approximately five minutes worth of scans (about 30 scans). All data collection was done during an active workday with people moving around the lab during the experiment.

We examined the spot-on accuracy of the stationary tablets during two periods: immediately after all of the rooms had been bound and 24 hours later. We report on the later data although the results were similar. We highlight three aspects of the results, shown in Table 1. First, in contrast to previous simulation results which found that Bayes with Gaussians exhibits accuracies above 95% (Haeberlen *et al.*, 2004), it had a spot-on hit rate of 82.5% in this more challenging live setting (*i.e.* the largest mean error). Second, as in the "nearby" experiment above, no algorithm was able to consistently differentiate between small, adjacent offices that had doors open to a common hallway (309, 310, 311, 312); the centroids of the rooms are about 2.5m apart. MAO with kernelised histograms and with a weak penalty for missing APs performed best, on average, but it could not consistently select the spot-on choice. If we examine the rooms that were selected, however, MAO with kernelised histograms did choose one of the four "nearby" rooms in 94.4% of cases, while the topmost Bayesian algorithm selected a nearby room in 88.3% of cases. We conjecture that it may be possible to reflect this uncertainty back to the user by highlighting a set of rooms instead of supplying only a single room as the result. Our third main result from this experiment was that MAO with weighted kernelised histograms together with a small penalty for missing APs performed best overall. In particular, it was significantly more stable throughout the lab and was 10% more accurate than Bayes with kernelised histograms, the current state-of-the-art.

5.3 *Motion Detection*

We wanted to examine the effect of using a motion detector to improve update lag and fingerprint clarity. Update lag occurs when a person moves from one room to another but the localiser does not reflect the new room immediately. This lag occurs because the localiser uses stale data: scans collected in a previous

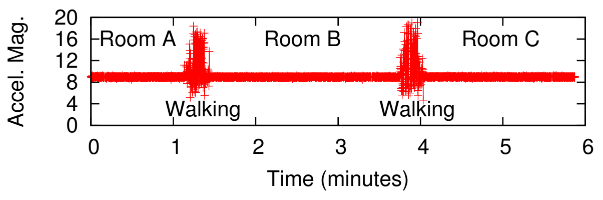

(a) Accelerometer Magnitude (at 10ms intervals)

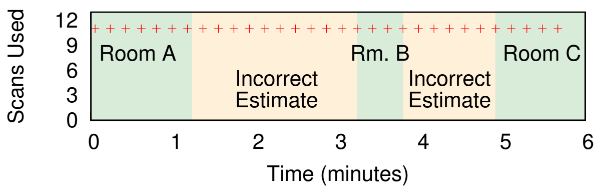

(b) Place estimates without motion detector

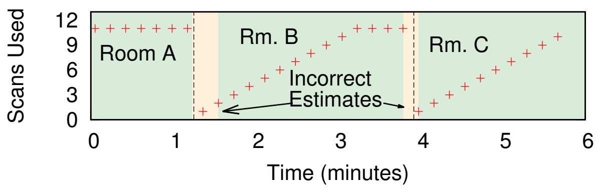

(c) Place estimates with motion detector

Figure 12. Using a motion detector to vary the number of scans used by the localiser significantly reduces update lag, presenting more up-to-date results to the user. Each + shows when the localiser received a new scan and produced a new estimate. The dashed line shows when the periodic motion detector determined that the user was walking.

room or while walking are still being used to form the estimate of the current location. We performed an experiment where we examined the use of a simple motion detector to expire old scans; the user's fingerprint repopulated with scans when the user stopped moving. Intuitively we would like to use as many scans as possible, but only if those scans come from the location the user is actually in.

Figure 12 illustrates how using a walk detector can significantly improve the user experience. In this experiment, we walked from room A to room B to room C, staying in room B for about two minutes. We logged the raw accelerometer readings at 10ms intervals (Figure 12a) and ran two instances of Molé on the same device, both running MAO with Gaussians. One instance did not use the motion detector and the other used the periodic motion detector described in Section 4.1, sampling for 0.5 seconds every 10 seconds. All fingerprints were cached and did not change during the experiment.

When Molé did not use a motion detector (Figure 12b), the estimate lagged behind the ground truth for one to two minutes because it used stale scans. When the instance running the motion detector detects motion (the dashed lines in Figure 12c), the localiser's scan queue is immediately truncated and there is far less delay before the correct space is chosen.

A second significant benefit to using a motion detector in a crowd-sourced positioning system is improved fingerprint clarity. In a crowd-sourced environment, a user can walk into a room, notice the estimate is incorrect, and immediately send a correcting bind. Unfortunately, this can lead to scans collected prior to the user entering the room becoming part of the fingerprint: a polluted fingerprint. To mitigate this problem, we truncate the on-device "bind" queue whenever walking is detected. This queue constitutes the scans that will be bound to the place if the user makes a correction.

To illustrate fingerprint pollution, we conducted the same "nearby" experiment as described in Section 5.2 only with the motion detector switched off. Figure 13 illustrates two instances where the fingerprint for Room R9, where the spot-check tablet is located, is polluted by binds in other rooms. When the roving tablet binds Room R7 for the second time at minute 20, we observe a shift in the estimates from R9 to R7. This occurred because many of the scans that were collected in Room R9 were not dropped when the user walked into Room R7, causing R7's fingerprint to become similar to R9's. The second instance is when Room R14 is bound at minute 39, soon after the user leaves the target room, R9. Again, this causes

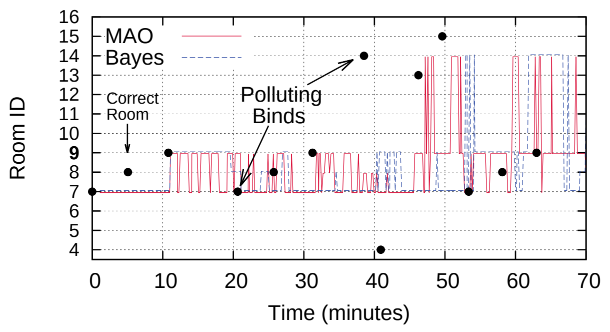

Figure 13. In a crowd-sourced positioning system without motion detection, fingerprints can easily become polluted with scans from old rooms. The data show that the two fingerprints of Rooms R7 and R14 erroneously acquired scans collected in Room R9, causing the estimate for R9 to vacillate with both positioning algorithms.

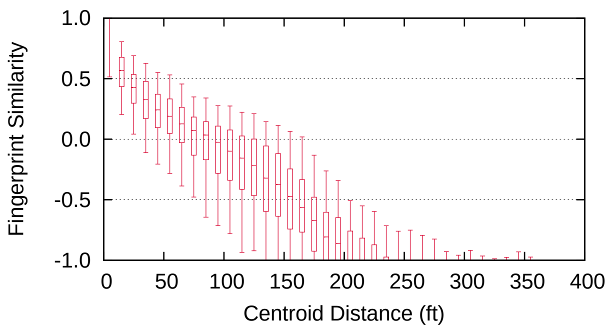

Figure 14. Fingerprint-to-Physical Distance Correlation. The data show that there is a strong correlation between fingerprint similarity and physical distance, particularly when spaces are nearby to one another. Physical distance is measured as centroid-to-centroid in a nine-story building which contains more than 1,400 distinct spaces. The top and bottom whiskers show the top 5% and bottom 5%, respectively. Box plot lines mark the 25^{th}, 50^{th}, and 75^{th} pcts.

R14 and R9 to erroneously have similar fingerprints, resulting in the localisers vacillating between several locations. As Figure 11 shows, *with* the motion detector switched on, fingerprints do not become polluted when new binds occur.

5.4 *Using Fingerprint Similarity*

One advantage of MAO as compared to Bayesian localisers is that it provides an abstract similarity function between any two fingerprints, either by using Equation 4 directly or by replacing $O(\cdot)$ with the overlap of the two histograms. Inferring physical distance from fingerprint distance has many uses, from the canonical "finding the nearest printer" to proximity-based notifications and device-pairing (Krumm and Hinckley, 2004).

By processing the scans from the 1,400 room building discussed above, we found that a useful correlation existed between the physical distance and fingerprint similarity across pairs of rooms. Using MAO with Gaussians, we show the correlation for this data set in Figure 14. Given objects or spaces tagged with fingerprints, this suggests that MAO can be used to estimate physical distances between them at a finer grain than simply observing that they can see the same MAC, for example. In this data set, spaces which had a fingerprint similarity > 0.5 were always less than 100 feet apart (closer spaces have a similarity nearer to 1). Because the fingerprint similarity computation is fairly trivial, it would also be possible to see if any k devices were likely to be within some physical distance of one another.

A second use for fingerprint similarity is that, even when the correct place is not the *most* similar to the user's fingerprint, it is almost always *one of* of the most similar. Because MAO returns a similarity score for each potential place, it is possible to look down the list of returned places beyond the top ranked place. Figure 15 shows that the correct place is almost always in the top four ranked places. In a visual map application, all of the highly ranked places could be highlighted if one did not stand out, assisting the user in making a correction.

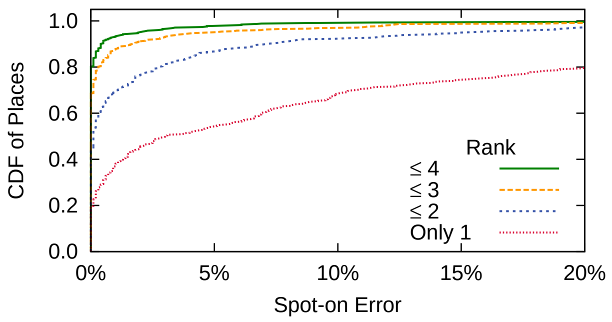

Figure 15. Many of the places in our data set are topologically close to one another. Topologically close places often have similar RF fingerprints, which occasionally confounds RF-based localisation. If we allow for non-exact matches, the data show that the true correct place is often only a few steps away from our best guess.

We foresee several algorithmic and user-facing uses for fingerprint similarity. First, similarity can be translated into degrees of proximity (e.g. nearby, distant). We have added a "proximity" user interface to Molé, allowing a user to see which other users are nearby (it is not enabled by default). Second, fingerprint similarity could be used to construct multiple fingerprints per space. Some "rooms" are, in fact, long hallways or large outdoor areas: a single fingerprint does not capture the signal variation throughout. By comparing binds for the same space, the Fingerprint Builder could decide to either merge them into a single fingerprint or to create an additional fingerprint associated with the same space. A final related use is outlier detection: if sets of scans linked to the same space are very different, an error condition can be raised, potentially lowering the confidence in other contributions by the same user. Evaluating uses of proximity and fingerprint similarity is future work.

5.5 *Crowd-sourcing Behavior*

For our last experiment, we wanted to understand whether Molé could be used by untrained participants. We first modified the user interface to include a positive feedback button ("Estimate OK"), signifying that the displayed estimate was, in fact, correct. We recruited four volunteers from Lab A; they had seen us testing Molé previously, but were otherwise untrained. Before giving the tablets to the volunteers, we performed one bind in Room R1 on an empty database. In effect, this initialized the hierarchy shown on all of the tablets so the volunteers would only need to edit the room label. They were given instructions to walk from room to room, fixing the estimate when it was wrong and clicking "Estimate OK" when it was correct. They were allowed to wait up to 30 seconds (three scans) for the estimate to become correct before marking "OK" and up to 60 seconds (six scans) before binding a correction.

In the middle of the workday, the volunteers then surveyed two floors for seventy minutes, splitting their time about 75/25 across the third and second floors, respectively (see Figure 9). Two of the meeting rooms, R14 and R17, were occupied during the experiment, and so were left unbound. Figure 16 shows how coverage and spot-on hit rate changed during the experiment. We calculated hit rate as a ten minute moving average of spot-on accuracy (*i.e.* when the volunteer clicked "Estimate OK"); this included the first bind for each room which is, by definition, an incorrect estimate. Once the rooms were surveyed after minute 50, the hit rate remained above 85% as it had done in our controlled experiments. No incorrect floor estimates were encountered. More qualitatively, the results show that a space shared by many people — approximately 150 people work on the two floors covered in the experiment — can be collaboratively surveyed by only a handful.

The volunteers provided us with feedback on Molé's usability and utility. They found the motion detector was occasionally not sensitive enough and that the device needed to be artificially shaken when it did not detect their walking (we had instructed them to do this). Because binds are sent to the server and not immediately applied to the binding client's area fingerprint cache (see Figure 4), there can be up to a twenty second delay in reflecting binds back to the user; several volunteers found this confusing. We plan on fixing this and the motion detector in upcoming versions. In general, the volunteers found Molé highly accurate, although they noticed the estimates were most often wrong in the same small, adjacent rooms

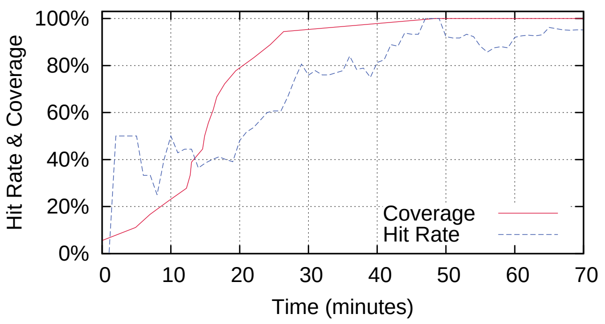

Figure 16. Four untrained volunteers were able to quickly survey a two story lab, with resulting accuracies above 85%. No floor errors were encountered.

we used for the "nearby" case (§ 5.2). They enthusiastically described several potential use cases such as navigating shopping malls, airports, and museums, finding promotions when shopping, and locating friends.

6 Related Work

Molé builds on two decades of prior work on positioning in GPS-less environments. Early systems, such as Active Badge (Want *et al.*, 1992) and Cricket (Priyantha *et al.*, 2000), used customized beacons and receivers, developing both main components of their respective positioning systems. As WiFi and cellular beacons have come to provide long-lived physical beacons at no additional infrastructure cost and as people have come to regularly carry personal mobile devices, the parameters of the indoor positioning problem have, in general, become more constrained: most research now assumes a fixed beaconing infrastructure is available, but whose main purpose is communication, not positioning. Since then, as first presented in the Radar project more than a decade ago (Bahl and Padmanabhan, 2000), researchers have tended to focus on two main approaches to GPS-less positioning: (a) a "radio map" approach, where first the position of the beacons is estimated, and then the position of the mobile device is "triangulated" using methods such as a RSSI-to-distance conversion (e.g. Griswold *et al.* (2004)) or angle-of-arrival (e.g. Niculescu and Badrinath (2003)), and (b) a "fingerprint" approach where the position of the beacons is ignored, and, instead, some method is used to select the best matching grid point or place from a database (e.g. Haeberlen *et al.* (2004)). Both of these broad classes require periodic surveying, which is typically a manual, laborious process and both classes have merit depending on the application. In general, the radio map approach is far more compact (its storage is O(radio beacons)), while the fingerprint approach is O(spaces). However, because of the confounding properties of varying building materials and multipath (Hashemi, 1993; Pahlavan *et al.*, 1998), most comparisons have found the fingerprint approach to be more accurate (e.g. ≈10m for the radio map of Griswold *et al.* versus a few meters for Haeberlen *et al.*). Very recent work using multiple antennae may again open up this question to debate (Xiong and Jamieson, 2012). Molé uses fingerprints for positioning (approach "b" above): end-users collect its fingerprints through crowd-sourcing, and it uses MAO for position estimation.

Haeberlen *et al.* (2004) suggested summarizing RSSI distributions with Gaussians. We used the overlap coefficient of pairs of Gaussian summaries, weighted by response rate, as one of MAO's localisers (we found that using the overlap of kernelised histograms provided superior accuracy, however). Lemelson *et al.* (2009) use unweighted Gaussian overlap – not to localise – but to anticipate the likely estimate localisation error for a given point. They show that points with very similar fingerprints (as determined by the overlap function) tend to have poor localisation accuracy, because they are often confused with adjacent points. An example where this method without the weighting would clearly perform poorly is a case where many spaces occasionally observe many APs, and always observe exactly one unique AP. In this case, the no-weighting method would lose the single unique characteristic in the noise, whereas the weighting method would select the right space. Although this is an extreme example, it illustrates a problem that often occurs in environments with dense but intermittent AP coverage. Our results show that Gaussian overlap with weighting is clearly superior to a weighting based on response rate, which performs the worst of the algorithms under test in Table 1.

The reponse rate of an AP, which MAO uses as a weighting function for its overlap coefficient, has also been considered as an altervative to RSSI measurements for RF-based localization. Cheng *et al.* (2005) explored the use of the reponse rate for 802.11-based localization in outdoor environments, showing that it has a strong correlation to the distance from the originating AP. Bargh and de Groote (2008) used the reponse rate for Bluetooth-based localization as an alternative to signal strengths, which is much more difficult to obtain on Bluetooth devices than on 802.11 devices. Relatedly, Letchner *et al.* (2005) use "negative information" — the absence of an AP — to bias the estimate toward places where that AP is absent. We showed in Section 5.1 how, because many APs may only be sensed from rarely in a given place, that this use of negative information is quite rigid and unlikely to give good results. In this work, we combined the response rate with the signal strength, achieving significant gain in localization accuracy compared to using the signal strength alone.

We showed how Molé varies the length of the localiser's scan queue to use many recent scans, but only if those scans are likely to be from the current place. Truncating the scan queue on movement detection also prevented bind pollution (§ 5.3). Several pieces of prior work have used accelerometer-based motion detection in location systems in different ways. Kim *et al.* (2010) use motion detection to save energy: after a user has arrived at a place and enough scans have been collected, and the variance in the motion detected is low enough, the WiFi radios are turned off. Once the motion variance exceeds its threshold, WiFi scanning is resumed. Shafer and Chang (2010) detect movement and, if walking is detected, perform what they refer to as a "full localisation," which presumably entails taking many scans over a short period after truncating the scan queue. If a user's walk is longer than the movement detection period, this can result in significantly more battery drain than our method because long series of scans will be repeatedly discarded. They also propose using low variance to detect idleness, choosing to scan slowly rather than switch off WiFi entirely. Bolliger *et al.* (2009) describe *asynchronous interval labeling* which allows sets of scans collected during the same stationary period to be retroactively bound at a more convenient time. Earlier, Krumm and Horvitz (2004) used WiFi, not accelerometers, to infer motion, using a hidden Markov model to identify motion and location simultaneously.

7 Conclusion

This article presented Molé, a mobile organic localisation engine, and focused primarily on its positioning algorithm MAO. In addition to MAO, we described in detail its hierarchical arrangement of places, which allows for unambiguous interpretation of users' location input, and its "cloud"-based server design, which improves scalability and privacy. Together, these components contribute to a positioning system that can run compactly on a broad range of mobile devices and scale worldwide. In particular, through controlled experiments and simulations, we showed that our localisation algorithm was 10% more accurate than the current state-of-the-art. This boost in accuracy occurred because we used discriminating information – a weighting based on response rate – that prior work had ignored. We also showed how the use of a motion detector can significantly reduce user-perceived estimation latency and eliminate bind pollution, where scans collected outside of a room spuriously become part of that room's fingerprint. Finally, we gave Molé to untrained users and found that they could quickly survey a medium-sized building, resulting in an accurate, shared location database that could be used for many applications.

In the future, we plan to extend the hierarchical and scalable structure of Molé to a visual map-based UI and to construct a browser plug-in version of Molé to work with more mobile devices and operating systems. We also plan to research combining slow background scans, an idleness detector, and a distinguishing MAO score to generate automatic binds that maintain an area's fingerprints as access points change over time due to maintenance events.

Acknowledgment

We thank the RVSN research group, especially Prof. Seth Teller, at MIT for their on-going collaboration and insights.

References

Bahl, P. and Padmanabhan, V.N., 2000. RADAR: An In-Building RF-Based User Location and Tracking System, *in: IEEE INFOCOM*, Tel Aviv, Israel, 775–784.

Bargh, M.S. and de Groote, R., 2008. Indoor Localization Based on Response Rate of Bluetooth Inquiries, *in: International Workshop on Mobile Entity Localization and Tracking in GPS-less Environments (MELT)*, San Francisco, CA, 49–54.

Barry, A., Fischer, B., and Chang, M., 2009. A Long-Duration Study of User-Trained 802.11 Localization, *in: International Workshop on Mobile Entity Localization and Tracking in GPS-less Environments (MELT)*, Orlando, FL, 197–212.

Bhasker, E.S., Brown, S.W., and Griswold, W.G., 2004. Employing User Feedback for Fast, Accurate, Low-Maintenance Geolocationing, *in: International Conference on Pervasive Computing and Communications (PerCom)*, Orlando, FL, 111–120.

Bolliger, P., 2008. RedPin: Adaptive, Zero-Configuration Indoor Localization, *in: International Workshop on Mobile Entity Localization and Tracking in GPS-less Environments (MELT)*, San Francisco, CA, 55–60.

Bolliger, P., Partridge, K., Chu, M., and Langheinrich, M., 2009. Improving Location Fingerprinting through Motion Detection and Asynchronous Interval Labeling, *in: Symposium on Location and Context Awareness (LoCA)*, Tokyo Japan, 37–51.

Charrow, B., 2010. *Organic Indoor Location: Infrastructure and Applications*, Master's thesis, Massachusetts Institute of Technology.

Cheng, Y.C., Chawathe, Y., LaMarca, A., and Krumm, J., 2005. Accuracy Characterization for Metropolitan-scale Wi-Fi Localization, *in: International Conference on Mobile Systems, Applications, and Services (MobiSys)*, Seattle, WA, 233–245.

Dong, F., Chen, Y., Liu, J., Ning, Q., and Piao, S., 2009. A Calibration-Free Localization Solution for Handling Signal Strength Variance, *in: International Workshop on Mobile Entity Localization and Tracking in GPS-less Environments (MELT)*, Orlando, FL, 79–90.

Ekahau, 2010. Ekahau Positioning Engine, `http://ekahau.com`, [Online; accessed 29-May-2012].

Griswold, W.G., Shanahan, P., Brown, S.W., Boyer, R.T., Ratto, M., Shapiro, R.B., and Truong, T.M., 2004. ActiveCampus: Experiments in Community-Oriented Ubiquitous Computing, *IEEE Computer*, 37 (10), 73–81.

Haeberlen, A., Flannery, E., Ladd, A.M., Rudys, A., Wallach, D.S., and Kavraki, L.E., 2004. Practical Robust Localization over Large-Scale 802.11 Wireless Networks, *in: International Conference on Mobile Computing and Networking (MOBICOM)*, Philadelphia, PA, 70–84.

Hashemi, H., 1993. Impulse response modeling of indoor radio propagation channels, *IEEE Journal on Selected Areas in Communications*, 11 (7), 967–978.

Inman, H.F. and Bradley, E.L., 1989. The Overlapping Coefficient as a Measure of Agreement between Probability Distributions, *Communications in Statistics-Theory and Methods*, 18 (10), 3851–3874.

Kim, D.H., Kim, Y., Estrin, D., and Srivastava, M.B., 2010. SensLoc: Sensing Everyday Places and Paths using Less Energy, *in: Embedded Networked Sensor Systems (SenSys)*, Zurich, Switzerland, 43–56.

Krumm, J. and Hinckley, K., 2004. The NearMe Wireless Proximity Server, *in: Ubiquitous Computing*, Nottingham, UK, 283–300.

Krumm, J. and Horvitz, E., 2004. LOCADIO: Inferring Motion and Location from Wi-Fi Signal Strengths, *in: International Conference on Mobile and Ubiquitous Systems (MobiQuitous)*, Cambridge, MA, 4–13.

Lemelson, H., Kjaergaard, M., Hansen, R., and King, T., 2009. Error Estimation for Indoor 802.11 Location Fingerprinting, *in: Symposium on Location and Context Awareness (LoCA)*, Tokyo Japan, 138–155.

Letchner, J., Fox, D., and LaMarca, A., 2005. Large-scale localization from wireless signal strength, *in: Twentieth National Conference on Artificial Intelligence*, Pittsburgh, Pennsylvania, 15–20.

Linacre, J.M., 1996. Overlapping Normal Distributions, *Rasch Measurement Transactions*, 10 (1), 487–488.

Madigan, D., Einahrawy, E., Martin, R.P., Ju, W.H., Krishnan, P., and Krishnakumar, A.S., 2005. Bayesian Indoor Positioning Systems, *in: IEEE INFOCOM*, Miami, FL, 1217–1227.

Niculescu, D. and Badrinath, B.R., 2003. Ad Hoc Positioning System (APS) Using AOA, *in: INFOCOM*, San Franciso, CA.

Pahlavan, K., Krishnamurthy, P., and Beneat, J., 1998. Wideband Radio Propagation Modeling for Indoor Geolocation Applications, *IEEE Communications Magazine*, 36, 60–65.

Park, J., Charrow, B., Curtis, D., Battat, J., Minkov, E., Hicks, J., Teller, S., and Ledlie, J., 2010. Growing an Organic Indoor Location System, *in: International Conference on Mobile Systems, Applications, and Services (MobiSys)*, San Francisco, CA, 271–284.

Park, J., Curtis, D., Teller, S., and Ledlie, J., 2011. Implications of Device Diversity for Organic Localization, *in: IEEE INFOCOM*, Shanghai, China, 3182–3190.

Priyantha, N., Chakraborty, A., and Balakrishnan, H., 2000. The Cricket Location-Support System, *in: International Conference on Mobile Computing and Networking (MOBICOM)*, Boston, MA, 32–43.

Shafer, I. and Chang, M.L., 2010. Movement Detection for Power-Efficient Smartphone WLAN Localization, *in: International Conference on Modeling, Analysis and Simulation of Wireless and Mobile Systems (WSWiM)*, Miami Beach, FL.

Want, R., Falcao, V., and Gibbons, J., 1992. The Active Badge Location System, *ACM Trans on Information Systems*, 10, 91–102.

Xiong, J. and Jamieson, K., 2012. Towards Fine-Grained Radio-Based Indoor Location, *in: International Workshop on Mobile Computing Systems and Applications (HotMobile)*, San Diego, CA.

Youssef, M. and Agrawala, A., 2005. The Horus WLAN Location Determination System, *in: International Conference on Mobile Systems, Applications, and Services (MobiSys)*, Seattle, WA.